Supplemental Material for

Constraining shallow S-wave velocity structure beneath the Azores-Madeira-Canaries region from Rayleigh-wave ellipticity analysis using UPFLOW data

Tae-shin Kim[1] ·Ana M. G. Ferreira[2] ·Glenn A. Jones[3] ·Sung-Joon Chang[1]

1 Interdisciplinary Program in Earth Environment System Science & Engineering, Kangwon National University, Chuncheon, South Korea

2 Department of Earth Sciences, University College London, London, United Kingdom

3 School of Earth and Environmental Sciences, Cardiff University, Cardiff, United Kingdom

Inversion

The 1-D shear wave velocity (Vs) profiles beneath each station were obtained by inverting the period-dependent ellipticity curves following the inversion scheme of Berbellini et al. (2019). Theoretical ellipticity curves were computed assuming fundamental-mode Rayleigh waves using the normal-mode summation approach implemented in the Computer Programs in Seismology software package (Herrmann, 2013).

The inversion was performed using the Neighbourhood Algorithm (NA; Sambridge, 1999), a self-adaptive Monte Carlo method that efficiently searches the model parameter space. The NA was configured with an initial random sampling of 1,000 models, followed by 20 new models generated per iteration, with the 5 best-fitting models selected to guide subsequent sampling. The misfit function minimised during the inversion is given by:

$$m = \sum_{i=1}^{N} \left(\frac{d_i - g_i(x)}{\sigma_D} \right)^2 \quad (1)$$

where d_i is the measured ellipticity, $g_i(x)$ is the predicted ellipticity for model x, σ_D is the measurement uncertainty, and N is the number of period-dependent measurements. The ensemble of models with misfit values within 20% of the minimum misfit was used to empirically quantify model uncertainty, with the uncertainty in Vs defined as the range of Vs across these ensemble models.

In addition to Vs, the input 1-D Earth model requires P-wave velocity (Vp) and density (ρ) profiles, which were estimated from Vs using empirical relations. For sedimentary layers, Vp was estimated from Vs using the empirical Vp-Vs relation for sediments of Castagna et al. (1985), and ρ was estimated from Vp using the relation of Hamilton (1979). For crustal layers, both Vp and ρ were estimated from Vs using the empirical relations of Brocher

(2005). The model parametrization consists of fixed numbers of sedimentary and crustal layers, with predefined ranges of layer thickness and Vs for each layer. A range of model parametrizations with differing numbers of sedimentary and crustal layers were tested for each station, and the optimal configuration was selected. The Vs and thickness ranges used in the final inversion are provided in Tables S1The maximum depth of the crustal layers was constrained such that the underlying mantle structure was fixed to the LITHO1.0 reference model (Pasyanos et al., 2014).

Table S1. Range of Vs values in km/s searched within each layer for each station considered in this study and corresponding layer thickness in km.

		J11D	J28D	UP40	UP38	UP02
Water layer	Vs	1.5				
	Thickness	0.0				
Sediment layer 1	Vs	0.1-1.5	0.1-1.0	0.1-2.0	0.1-2.0	0.0-1.0
	Thickness	0.01-3.0	0.01-1.0	0.01-3.0	0.01-3.0	0.0-1.0
Sediment layer 2	Vs				0.1-2.0	
	Thickness				0.01-3.0	
Crust layer 1	Vs	1.5-3.2	1.0-3.0	2.0-3.0	2.0-2.9	0.0-4.5
	Thickness	0.1-3.0	0.1-2.5	0.1-5.0	0.1-7.0	3.0-15.0
Crust layer 2	Vs	3.2-4.0	3.0-4.0	3.0-4.0	2.9-4.0	
	Thickness	1.5-5.0	2.5-6.0	3.0-10.0	0.1-10.0	

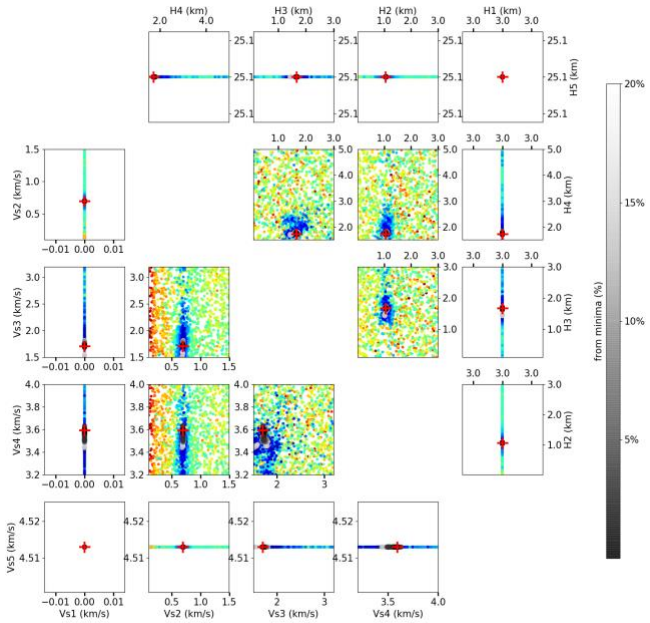

Figure S1. Scatter plots and distributions of Vs and layer thickness for each layer at station J11D. The best-fitting solution is marked by red crosses. Parameters corresponding to models within 20% of the best-fitting solution are shown in black and gray.

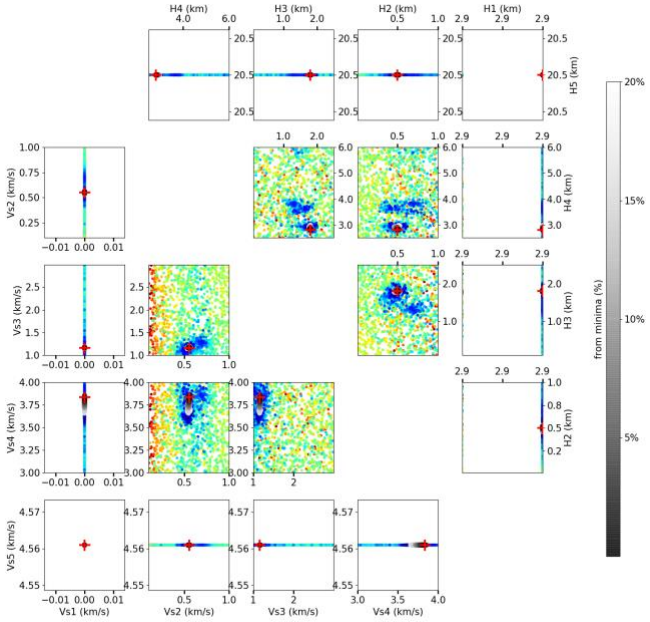

Figure S2. Same as Fig. S1 but for station J28D.

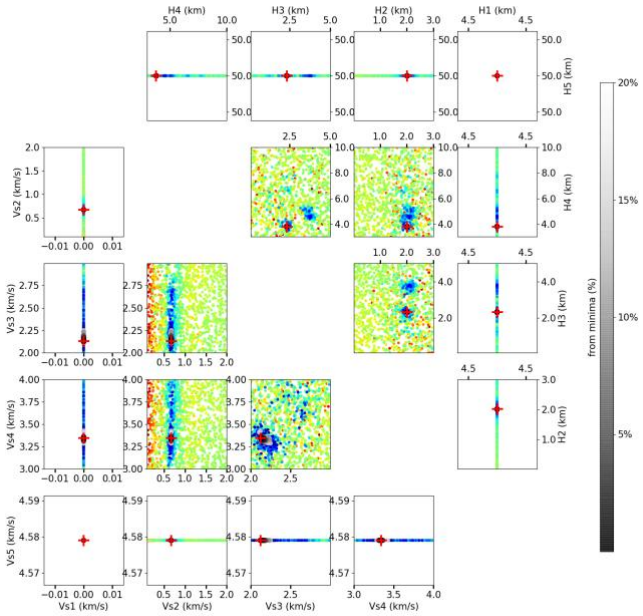

Figure S3. Same as Fig. S2 but for station UP40.

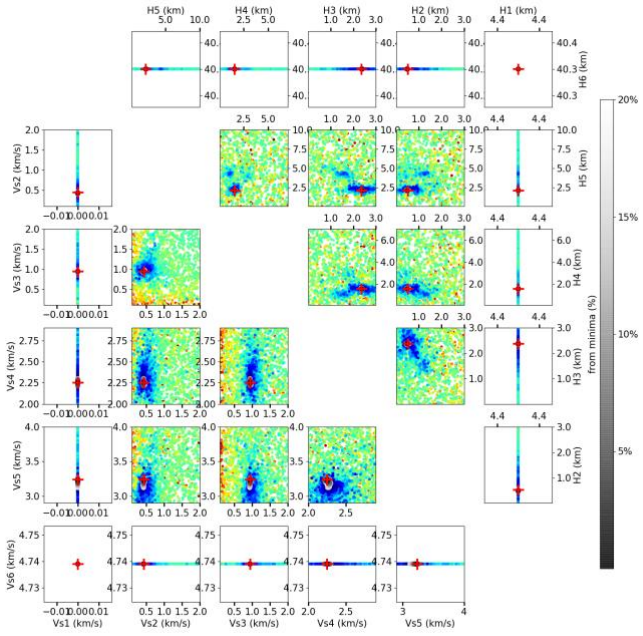

Figure S4. Same as Fig. S3 but for station UP38.

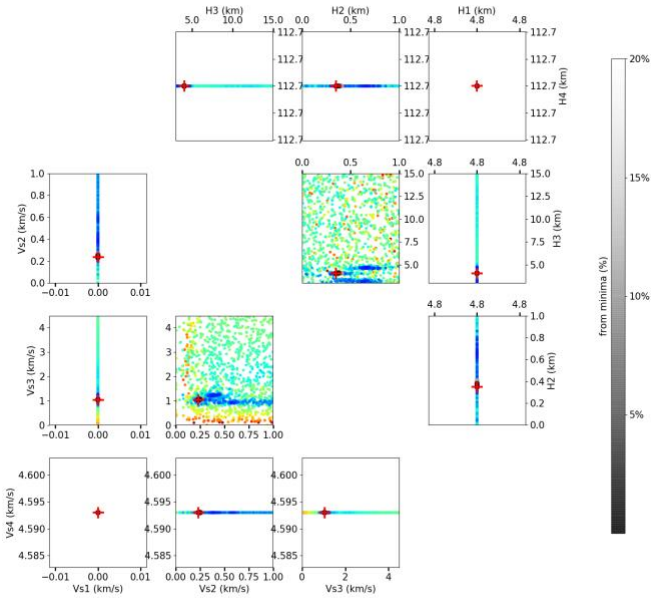

Figure S5. Same as Fig. S4 but for station UP02.

References

Berbellini, A., Schimmel, M., Ferreira, A. M. & Morelli, A. Constraining S-wave velocity using Rayleigh wave ellipticity from polarization analysis of seismic noise. Geophys. J. Int. 216, 1817–1830 (2019).

Brocher, T. M. Empirical relations between elastic wavespeeds and density in the Earth's crust. Bull. Seismol. Soc. Am. 95, 2081–2092 (2005).

Castagna, J.P., Batzle, M.L. & Eastwood, R.L. Relationship between compressional-wave and shear-wave velocities in clastic silicate rocks, Geophysics, 50, 571–581 (1985).

Hamilton, E.L. Vp/Vs and Poisson's ratios in marine sediments and rocks, J. Acoust. Soc. Am., 66 (4), 1093–1101 (1979).

Herrmann, R. B. Computer programs in seismology: An evolving tool for instruction and research. Seismol. Res. Lett. 84, 1081–1088 (2013).

Pasyanos, M. E., Masters, T. G., Laske, G. & Ma, Z. LITHO1. 0: An updated crust and lithospheric model of the Earth. J. Geophys. Res.: Solid Earth 119, 2153–2173 (2014).

Sambridge, M. Geophysical inversion with a neighbourhood algorithm—I. Searching a parameter space. Geophys. J. Int. 138, 479–494 (1999).